



## Pharmacology

# Plasma and cerebrospinal fluid population pharmacokinetic modeling and simulation of meropenem after intravenous and intrathecal administration in postoperative neurosurgical patients

Xingang Li <sup>a,b</sup>, Xiaoping Wang <sup>c</sup>, Yuanxing Wu <sup>d</sup>, Shusen Sun <sup>e</sup>, Kai Chen <sup>f</sup>, Yanxia Lu <sup>g,\*</sup>, Qiang Wang <sup>f,\*</sup>, Zhigang Zhao <sup>a,b,\*</sup>

<sup>a</sup> Department of Pharmacy, Beijing Tiantan Hospital, Capital Medical University, Beijing, 100050, China

<sup>b</sup> Precision Medicine Research Center for Neurological Disorders, Beijing Tiantan Hospital, Capital Medical University, Beijing, 100050, China

<sup>c</sup> Department of Pharmacy, Shaanxi Provincial Hospital of Traditional Chinese Medicine, Xian, 710003, China

<sup>d</sup> Respiratory and Critical Care Medicine, Beijing Anzhen Hospital, Capital Medical University, Beijing, 100050, China

<sup>e</sup> College of Pharmacy, Western New England University, Springfield, MA 01119, USA

<sup>f</sup> Intensive Care Unit, Beijing Tiantan Hospital, Capital Medical University, Beijing, 100050, China

<sup>g</sup> Department of Pharmacy, The General Hospital of the Chinese People's Armed Police Forces, Beijing, 100039, China

## ARTICLE INFO

## Article history:

Received 6 July 2017

Received in revised form 2 July 2018

Accepted 12 August 2018

Available online 17 August 2018

## Keywords:

Meropenem

Population pharmacokinetics

Cerebrospinal fluid

Drainage

Intracranial infections

Craniotomy

## ABSTRACT

Combined intravenous and local intrathecal administration of meropenem in patients after craniotomy is widely used to treat intracranial infections. However, the optimal dosing regimen of meropenem has not been investigated, posing a risk to treatment efficacy. We aimed to identify significant factors associated with inter-individual variability in cerebrospinal fluid (CSF) pharmacokinetics of meropenem and to evaluate potential intravenous and intrathecal meropenem dosing regimens for the treatment of patients with intracranial infections. After the diagnosis of intracranial infection, 15 patients with an indwelling drain tube received intravenous and intrathecal administration of meropenem. Blood and cerebrospinal fluid (CSF) samples were obtained at the scheduled time to measure meropenem concentration. Plasma and CSF concentration-time data were fit simultaneously using a nonlinear mixed-effects modeling approach. A 3-compartmental model was selected to characterize the in vivo behavior of meropenem. Through population modeling, multiple covariates were tested about their impact on the meropenem pharmacokinetics. Considering CSF outflow via drain tube leading to a drug loss, the drug clearance in CSF ( $CL_{CSF}$ ) was added to describe this drug loss. The covariate selection indicated that the drainage volume (mL/d) had a significant positive correlation with  $CL_{CSF}$ . Bootstrap and visual predictive check suggested a robust and reliable pharmacokinetic model was structured. The established final population model was useful to apply with simulation to identify meropenem dosing regimens for the treatment of patients with intracranial infections. With the goal of CSF concentrations exceeding the minimum inhibitory concentration during the therapy, we created a simple to use dosage regimen table to guide clinicians with drug dosing.

© 2018 Published by Elsevier Inc.

## 1. Introduction

Postoperative intracranial infection, which may present as a life-threatening emergency, is a common complication in neurosurgery (National Nosocomial Infections Surveillance, 2004). Meropenem is a potent broad-spectrum carbapenem with potent in vitro activity against gram-negative bacilli, gram-positive cocci, and anaerobic bacteria. Meropenem 2 g every 8 hours (q8h) is commonly used in the treatment of patients with intracranial infections (Beer et al., 2008; Tunkel et al.,

2004). Because the blood–brain barrier (BBB) is disrupted by neurosurgery, meropenem could penetrate into the cerebrospinal fluid (CSF) from the blood (Zhang et al., 2017). However, a high inter-individual variability (IIV) in the degrees of BBB damage results in an unreliable permeability through the disrupted BBB (Blassmann et al., 2016; Lu et al., 2016; Zhang et al., 2017). For example, a higher dosage is needed to obtain sufficient CSF concentrations in a patient with less BBB damage. After a craniotomy, external CSF drainage is often used to drain CSF from the operational cavity, ventricles of the brain, or the lumbar subarachnoid space to a drainage bag (Chung et al., 2017b; Shi et al., 2017). To achieve a reliable CSF concentration, a local intrathecal route of administration through CSF drainage is often utilized in clinical practice (Remes et al., 2013; Shofty et al., 2016; Tsimogianni et al., 2017).

\* Corresponding authors.

E-mail addresses: [lyx\\_67386@sina.com](mailto:lyx_67386@sina.com) (Y. Lu), [tyyqwq@163.com](mailto:tyyqwq@163.com) (Q. Wang), [1022zzg@sina.com](mailto:1022zzg@sina.com) (Z. Zhao).

However, little is known about the plasma and CSF population pharmacokinetics after intravenous and intrathecal administration in post-operative neurosurgical patients. The optimal local dose of meropenem has not been investigated. This study was designed to identify significant factors associated with IIV in CSF pharmacokinetics of meropenem and to evaluate potential intravenous and intrathecal meropenem dosing regimens for the treatment of patients with intracranial infections.

## 2. Methods

### 2.1. Patient selection

This study was conducted at the Beijing Tiantan Hospital Affiliated to Capital Medical University, China. Postoperative neurosurgical patients with indwelling drainage tubes were admitted to the intensive care unit. All patients were diagnosed with an intracranial infection, based on following criteria (Wu et al., 2017): (1) changes in CSF specimens: white blood cell count  $>1000 \times 10^6$  cells/L, CSF glucose  $<40\%$  of serum glucose or  $<2.2$  mmol/L; and (2) temperature  $<36^\circ\text{C}$  or  $>38^\circ\text{C}$ , positive signs of headache, vomiting, and meningeal irritation (nuchal rigidity, Kernig sign and Brudzinski sign). Patients with a history of meropenem allergy, deep coma, and agonal state were excluded from this study.

### 2.2. Study design

All enrolled patients received both intravenous and intrathecal meropenem for treatment of intracranial infection. Meropenem 2000 mg was dissolved in 250 ml of 0.9% normal saline solution. Meropenem 10 mg was administered via the drainage tube, and flushed with about 2 mL saline solution to ensure the entire dose was infused. The drainage tube was clamped off for 15 minutes and then reopened for drainage. The remaining 1990 mg of meropenem was given intravenously over 1 h with a syringe pump (1990 mg/h). Patients were dosed in the same fashion every 12 h. After 48 h, CSF samples (about 1.5 mL, from the drainage tube) and venous blood specimens (about 2.5 mL, from the arm without the intravenous infusion) were collected at scheduled times [48 h (pre-dose), 48.25, 48.5, 49, 51, 53, 56, and 60 h] after meropenem administration. CSF and blood specimens were separated by centrifugation at  $3500 \times g$  and  $8500 \times g$  for 5 min, respectively. Supernatants of CSF and plasma were then suctioned and preserved at  $-80^\circ\text{C}$  until analyzed. A previously reported HPLC method was used to determine supernatant meropenem concentrations. The method was accurate given high intra- and inter-assay precision,  $<13.5\%$  for plasma samples and  $<12.9\%$  for CSF samples, with linear calibration curves ranging from 2 to 200 mg/L.

This study protocol was approved by the Institutional Review Board of Beijing Tiantan Hospital, Capital Medical University (ID: KY2014–014–02). Written informed consents were obtained from all patients or their healthcare surrogates.

### 2.3. Structural model development

The meropenem pharmacokinetics were described using simple compartmental models. The disposition of meropenem in blood was characterized by a two compartment model (Ohata et al., 2011; Usman et al., 2017). Because of the disruption of the BBB after neurosurgery, meropenem can penetrate into the CSF easily. Therefore, the disposition of meropenem in CSF was described using a single compartment model (Lu et al., 2016). The drug distribution among compartments was characterized by the first-order process. Since CSF outflowing through the drainage tube results in measurable drug loss, this was proposed to be the main elimination pathway of CSF drug. Therefore, another parameter of the clearance of the CSF compartment ( $CL_{\text{CSF}}$ ) was incorporated into the model to describe this elimination.

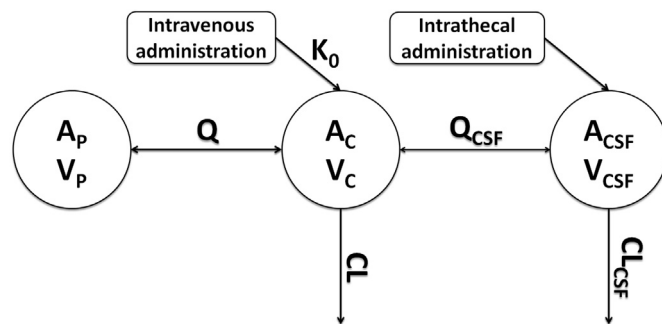


**Fig. 1.** The proposed pharmacokinetic structural model of meropenem in intracranial infection patients with an indwelling drain in the operational area/ventricle. Patients received both intravenous and intrathecal administration of meropenem twice a day.  $A_C$  = drug amount in the central compartment;  $V_C$  = central volume;  $A_P$  = drug amount in the peripheral compartment;  $V_P$  = distribution volume of the peripheral compartment;  $A_{\text{CSF}}$  = drug amount in the CSF compartment;  $V_{\text{CSF}}$  = distribution volume of the CSF compartment;  $Q$  = inter-compartment clearance between the central and peripheral compartment;  $Q_{\text{CSF}}$  = inter-compartment clearance between the central and CSF compartment;  $CL$  = clearance of the central compartment;  $CL_{\text{CSF}}$  = clearance of the CSF compartment. Eqs. (1) to (3) outlined in the manuscript were used to describe this model.

The schematic diagram is shown in Fig. 1 and the differential Eqs. (1–3) are as follows:

$$\frac{dA_C}{dt} = K_0 - Q \times (C_C - C_P) - Q_{\text{CSF}} \times (C_C - C_{\text{CSF}}) - CL \times C_C \quad [A_{C,0} = 0] \quad (1)$$

$$\frac{dA_P}{dt} = Q \times (C_C - C_P) \quad [A_{P,0} = 0] \quad (2)$$

$$\frac{dA_{\text{CSF}}}{dt} = Q_{\text{CSF}} \times (C_C - C_{\text{CSF}}) - CL_{\text{CSF}} \times C_{\text{CSF}} \quad [A_{\text{CSF},0} = 10 \text{ mg}] \quad (3)$$

$$C_C = \frac{A_C}{V_C} \quad (4)$$

$$C_P = \frac{A_P}{V_P} \quad (5)$$

$$C_{\text{CSF}} = \frac{A_{\text{CSF}}}{V_{\text{CSF}}} \quad (6)$$

$A_C$ ,  $A_P$ , and  $A_{\text{CSF}}$ , respectively, represents the drug amount in the central, peripheral and CSF compartments.  $A_{C,0}$ ,  $A_{P,0}$ , and  $A_{\text{CSF},0}$  are the initial drug amounts in the central, peripheral, and CSF compartment, respectively.  $K_0$  is the intravenous rate (1990 mg/h). The definition of the pharmacokinetic parameters ( $Q$ ,  $Q_{\text{CSF}}$ ,  $V_C$ ,  $V_P$ ,  $V_{\text{CSF}}$ ,  $CL$  and  $CL_{\text{CSF}}$ ) can be found in Fig. 1.

### 2.4. Population pharmacokinetic model

The population pharmacokinetic model was developed using non-linear mixed-effects modeling method. Plasma and CSF concentrations were fitted simultaneously using Phoenix NLME software (Version 7.0, Certara, St. Louis, Missouri) with the First Order Conditional Estimation - Extended Least Squares (FOCE-ELS) method (Li et al., 2017). Pharmacokinetic parameters' inter-individual variability ( $\eta$ ) was assumed to follow a log-normal distribution with a mean of zero and a variance of  $\omega^2$  (Eq. (7)).

$$P_i = P \times e^{\eta_i} \quad (7)$$

where  $P_i$  and  $P$  are the individual parameter and population typical parameter, respectively. The proportional error model was used to describe the random error model. The random error ( $\varepsilon$ ) was assumed to

follow a normal distribution with mean of 0 and a variance of  $\sigma^2$  (plasma concentration:  $\sigma_1^2$ , CSF concentration:  $\sigma_2^2$ ).

$$C_{CI} = C_C \times (1 + \varepsilon_1) \quad (8)$$

$$C_{CSFi} = C_{CSF} \times (1 + \varepsilon_2) \quad (9)$$

A covariate analysis was undertaken to evaluate the impact of covariates on pharmacokinetic parameters. In this dataset, both categorical covariates (sex and drainage position) and continuous covariates [age (year), body weight (kg), creatinine clearance ( $CL_{CR}$ , ml/min, estimated using the Cockcroft–Gault equation), CSF albumin (mg/dL) and drainage volume (mL/d)] were included. The effect of the categorical covariate on each parameter was assessed using a proportional shift function. Continuous covariates were centered at their median values, and the impact of each covariate on parameters was evaluated using linear, exponential and power functions. Forward inclusion [ $P < 0.01$ , the decrease of objective function (OFV) values  $> 6.64$ ] followed by the backward elimination ( $P < 0.001$ , the increase of OFV values  $> 10.83$ ) was applied to establish the final population pharmacokinetic model.

### 2.5. Model evaluation and validation

Visual evaluation methods (goodness-of-fit plots) were applied to evaluate the reliability of both the base structural model and the final model. Goodness-of-fit plots included four scatter plots: conditional weighted residual errors (CWRES) versus time after dose, CWRES versus population predictions, observations against population predictions, observations and population predictions against time after dose. Both the bootstrap resampling methodology and visual predictive checks (VPCs) were used to assess the stability and predictive performance of the final model (Li et al., 2015, 2016). One thousand datasets were generated with different combinations of patients using random sampling with replacement, and the parameters were re-estimated using the final population model. Median parameter values along with their 95% confidence intervals (95%CI, 2.5th and 97.5th percentiles of the 1000 bootstrap-estimated parameters) from bootstrap estimates were compared with the estimates of the final model. In addition, simulations of 1000 virtual datasets were performed based on the final population model. The observations were overlaid on the 5th, median, and 95th percentiles (90% prediction intervals, 90% PI) of simulations. The final VPCs plots were grouped by plasma and CSF concentrations.

### 2.6. Simulation

The primary objective of the simulations was to provide dosing guidance for the use of meropenem in postoperative neurosurgery patients. Given that CSF represented the effect site of interest, CSF drug concentrations were evaluated. To calculate the penetration ratio, the external CSF drainage was turned off ( $CL_{CSF}$  set to 0), so that the disposition of meropenem in the CSF is only attributed to by distribution from the plasma compartment through the BBB. Monte Carlo simulations (1000 patients) were performed. As meropenem is considered to be time-dependent, the percentage of the dosing interval that drug concentrations are above the minimum inhibitory concentration (MIC,  $T > MIC$ ) is the pharmacokinetic/pharmacodynamic (PK/PD) index associated with antimicrobial activity. The free-drug meropenem concentration in blood was corrected by a protein binding rate of 2%, while it was assumed that all meropenem in CSF is free (Lu et al., 2016). Considering the severity of infection, the goal meropenem dose administration was to achieve CSF concentrations exceeding the MIC for the entire dosing interval ( $\%T > MIC$ ) (Li et al., 2007; Li et al., 2018). Using the final population pharmacokinetic model, we calculated the drug concentration data at different times based on the relationship between pharmacokinetics parameters and the covariates. The deterministic simulations were performed in which the typical values were fixed to the final

parameter estimates and IIV was fixed to zero. Patients were divided into different subgroups according to covariates significantly associated with pharmacokinetics. Simulations were conducted using the Phoenix NLME software to find the optimal individualized dosing regimen for different subgroups of patients. A simple to use dosage regimen table was derived based on the results of simulations.

## 3. Results

### 3.1. Patient characteristics

A total of 15 patients with intracranial infection (9 males and 6 females) were enrolled in this study. Information about diagnosis, age (year), body weight (kg), serum creatinine ( $\mu\text{mol/L}$ ), CSF albumin (mg/dL), drainage position, CSF white blood cell (WBC, cells/ $\mu\text{L}$ ), CSF glucose (mmol/L), and drainage volume (mL/d) for each patient were retrieved from medical records and are listed in the Supplemental material 1. Although we attempted to collect all CSF and blood specimens at the scheduled times, certain specimens were not able to be collected, mainly due to the postoperative patients' frail physical condition at the time of the blood and CSF sample collections. In total, 102 plasma and 82 CSF samples were obtained for concentration determination and pharmacokinetic analysis. All patients were treated empirically with meropenem and information about the bacterial species was not captured. All patients were considered to be cured based on the evaluations of their symptoms, laboratory tests and the eradication of bacterial pathogens.

### 3.2. Final model

Creatinine clearance is a well-known covariate influencing meropenem clearance (Chung et al., 2017a; Tsai et al., 2016; Usman et al., 2017). Since the enrolled patients demonstrated normal kidney function, creatinine clearance was not incorporated in the final population model. Body weight was also not added in the final model due to its narrow distribution. After forward-inclusion and backward elimination processes, covariate drainage volume (mL/d) was identified and included in the final population pharmacokinetic model. A significant positive correlation was observed between the drainage volume and  $CL_{CSF}$ . Their relationships in the final model were described by the following equation:

$$CL_{CSF} \left( \frac{L}{h} \right) = 0.027 \times [1 + (\text{Drainage volume} - 175)] \times 0.017 \times e^{\eta_{CL_{CSF}}} \quad (10)$$

where 0.027 L/h is the typical value of  $CL_{CSF}$  when the drainage volume is 175 mL/d, and 0.017 represents the estimated coefficient describing the association between the drainage volume and  $CL_{CSF}$ ; 175 mL/d represents the median value of the drainage volume.  $\eta_{CL_{CSF}}$  represents the inter-individual variability of  $CL_{CSF}$ . According to this equation,  $CL_{CSF}$  increases with an increase of the drainage volume. The parameter estimates of the final population pharmacokinetic model are listed in Table 2. All parameters were estimated with an acceptable precision [relative standard error (RSE) with ranges from 7.82% to 34.48%].

### 3.3. Goodness-of-fit and model validation

Goodness-of-fit plots of the basic pharmacokinetic model and the final model are displayed in Fig. 2. Observations and population predictions versus time (Fig. 2A and A') allowed for evaluation of the model. Both CWRES versus time and CWRES versus population predictions (Fig. 2B, C, B' and C') were applied to detect any misspecifications in base and final models. The scatter plots between observations and population predictions were compared between base and final models (Fig. 2D and D'). In the final model, drainage volume was added to parameter  $CL_{CSF}$ , and  $CL_{CSF}$  had a significant impact on the CSF concentration. The prediction of CSF concentration was improved significantly. No

apparent systematic bias was observed in these plots. The proposed final model described meropenem pharmacokinetics in enrolled patients appropriately. The plots of individual fits are displayed in the Supplemental material 2.

Bootstrap results of median parameter estimates with 95%CI are listed in Table 1. The median values are similar to the original parameter estimates, and the 95% CIs enclose the values estimated during data fitting. Bootstrap shows an acceptable robustness of the final population pharmacokinetic model. Meropenem VPCs plots showed the 90% prediction intervals (90% PI) and the actual observations (grouped by plasma and CSF concentrations) (Fig. 3). The dashed lines represent

5th and 95th percentiles and the solid lines represent predicted 50th percentile. The area between the 5th and 95th percentiles represents the 90% PI. 92.9% (171/184) of the observations stay within the 90%PI, suggesting adequate predictive properties of the final population model.

3.4. Simulation

We calculated the CSF penetration ratio, and mean ± standard deviation of CSF penetration ratio are 0.29% ± 0.10%. Since only one covariate (drainage volume) was incorporated in the final model, patients

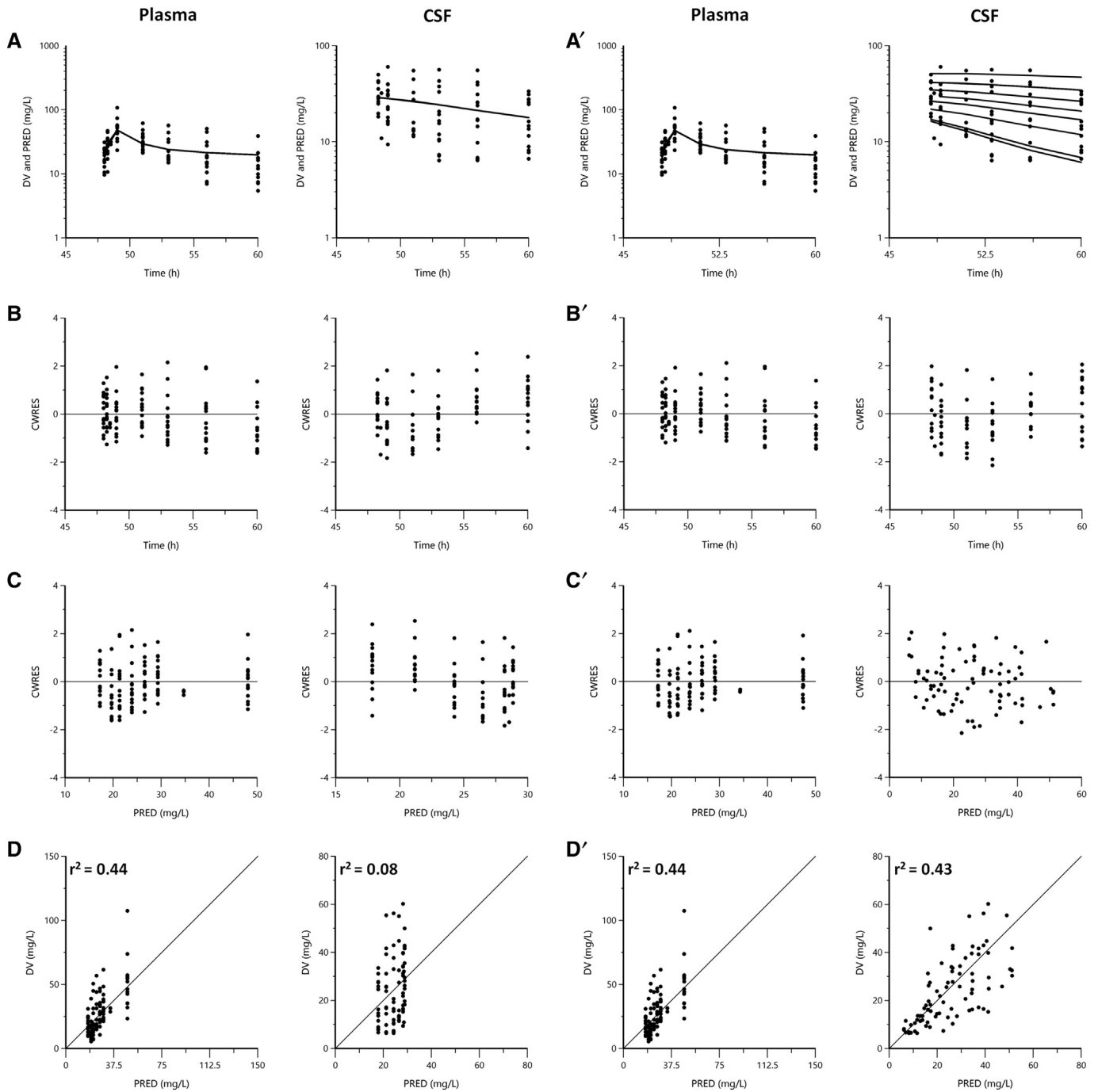


**Fig. 2.** The goodness-of-fit plots of basic (A–D) and final (A’–D’) population pharmacokinetic models. A and A’: observations (dots) and population predictions (lines) against time. There are multiple lines for the CSF observations versus predictions plot, and each line represents predictions based on a specific drainage volume (based on available drainage volume provided in the analysis data); B and B’: conditional weighted residuals (CWRES) versus time; C and C’: CWRES versus population predictions; D and D’: observations versus population predictions and the lines represent the lines of unity  $y = x$ .  $r^2$ : coefficient of determination of linear regression.

**Table 1**  
Parameter estimates and bootstrap results of meropenem population pharmacokinetic model in postoperative neurosurgical patients with intracranial infections.

| Parameter        | Model estimates |       |       |             |          | Bootstrap results |             |          |
|------------------|-----------------|-------|-------|-------------|----------|-------------------|-------------|----------|
|                  | Estimate        | Units | RSE%# | 95% CI      | IIV(CV%) | Median            | 95%CI       | IIV(CV%) |
| $V_C$            | 50.34           | L     | 13.85 | 36.57–64.10 | 28.37    | 49.60             | 33.49–65.71 | 29.37    |
| CL               | 4.56            | L/h   | 10.61 | 3.60–5.51   | 0.03     | 4.49              | 3.40–5.59   | 0.03     |
| $V_{CSF}$        | 0.88            | L     | 16.24 | 0.60–1.17   | 71.01    | 1.00              | 0.62–1.38   | 66.21    |
| $CL_{CSF}$       | 0.027           | L/h   | 13.02 | 0.020–0.034 | 0.74     | 0.028             | 0.021–0.036 | 2.59     |
| $Q_{CSF}$        | 0.029           | L/h   | 34.48 | 0.009–0.050 | 1.26     | 0.026             | 0.016–0.037 | 1.39     |
| $V_P$            | 70.99           | L     | 18.39 | 45.40–96.58 | 59.53    | 74.43             | 52.49–96.38 | 70.83    |
| Q                | 23.97           | L/h   | 19.82 | 14.59–33.35 | 54.51    | 22.20             | 8.60–35.80  | 56.92    |
| $f_{DV-CLCSF}^*$ | 0.017           |       | 25.78 | 0.008–0.026 | -        | 0.016             | 0.008–0.024 | -        |
| $\sigma_1$       | 37              | -     | 7.82  | 31–42       | -        | 36                | 31–42       | -        |
| $\sigma_2$       | 30              | -     | 11.19 | 23–36       | -        | 35                | 27–42       | -        |

\*  $f_{DV-CLCSF}$  = coefficient representing the relationship between the drainage volume and  $CL_{CSF}$ .

# RSE = relative standard error.

were categorized by the drainage volume (<100 mL/d, 100–200 mL/d, 200–300 mL/d and 300–400 mL/d). The range of drainage volumes during simulation were restricted to the ranges observed in the modeled data to prevent distortion of results. The values of  $CL_{CSF}$  were calculated using Eq. (10) and the other parameters were fixed as the population typical values and random variability was fixed to zero. With the goal of having CSF concentrations be above the MIC during the therapy (100% T > MIC), the optimal intravenous dose (1 h infusion) and local doses for different subgroups of patients are listed in Table 2. To assess the recommended dosing regimens, we performed Monte Carlo simulations with 1000 simulated patients (IIV implemented), and determined the percent probabilities of PK/PD target attainment based on a % T > MIC target of 100% by drainage volume and MIC values. The dosing regimens by drainage volume and MIC value associated with the percent probabilities of PK/PD target attainment of at least 80% are shown in Table 2. The actual percent probabilities of PK/PD target attainment achieved for each dosing regimen by drainage volume and MIC value are shown in Table 3. The results of this simulation only apply to patients whose drainage volumes were within the ranges observed in the modeled data. Both intravenous infusion and local administration were Q12h dosing. Simulation results showed that as MIC and daily CSF drainage volume increase, intravenous and local doses needed to be increased as well to maintain optimal exposures.

#### 4. Discussion

The inter-individual variability of CSF concentration may be partly ascribed to the contribution of different degrees of BBB disruption (Li et al., 2018; Lu et al., 2016). A local intrathecal route of administration through CSF drainage is one dosing strategy to achieve a sufficient CSF meropenem concentration (Segal-Maurer et al., 1999). After combined intravenous and intrathecal administration, we found that the highest CSF trough concentration was greater than 33 mg/L and lowest concentration was about 6 mg/L. To date, the optimal local dose of meropenem has not been investigated. Based on our clinical experience, we chose to administer 10 mg of meropenem to the study patients. This study aimed to identify factors affecting CSF concentration and provide optimal dosing regimens for this specific population. Nonlinear mixed-effects modeling method was applied to develop the population pharmacokinetic model, and the covariate analysis identified that the drainage volume (mL/d) had a significant negative correlation with the CSF concentration. To the best of our knowledge, this is the first report to evaluate the plasma and CSF pharmacokinetic profile of meropenem through population modeling and simulation after both intravenous and intrathecal administration in postoperative neurosurgical patients.

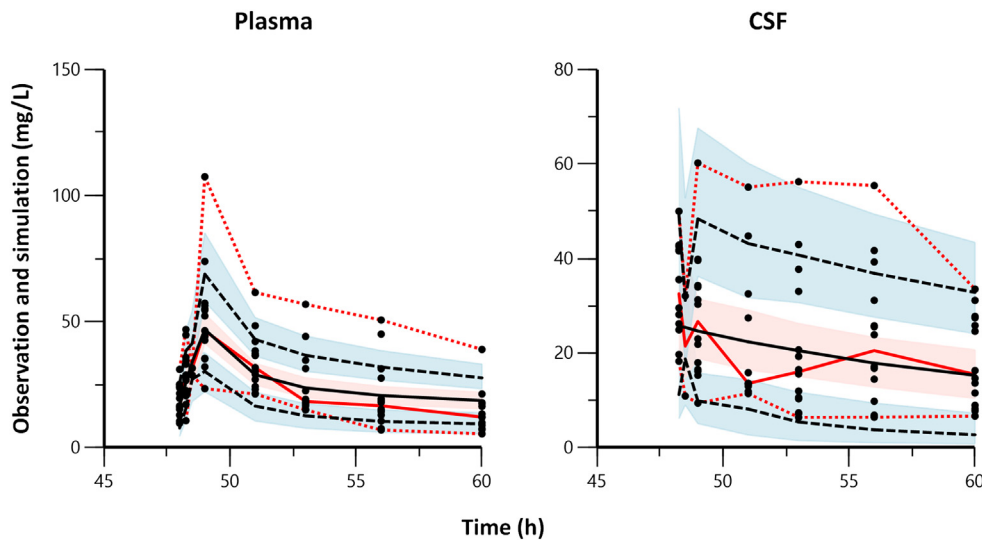


**Fig. 3.** The visual predictive check plots from the final population pharmacokinetic model. The dots are the actual original observations. The black dashed lines are the 5%, and 95% quantiles and the black solid lines represent 50% quantiles from the simulated observations. The red shaded area represents the 95% confidence intervals for the model predicted 50% quantile. The blue shaded areas represent the 95% confidence intervals for the model predicted percentiles 5th and 95th quantiles. The solid red line represents the 50% quantile from the observations. The observed 5th and 95th quantiles are presented with red dashed lines.

**Table 2**

Meropenem dosing regimens for postoperative neurosurgical patients with intracranial infections based on the drainage volume and MIC (100% T > MIC, ~80% of patient population).

| Drainage volume (ml/d) | Meropenem dosage regimen [IV dose (mg) + local dose (mg)]* |              |              |               |
|------------------------|--|--------------|--------------|---------------|
|                        | MIC <sup>#</sup> = 2 mg/L                                  | MIC = 4 mg/L | MIC = 8 mg/L | MIC = 16 mg/L |
| <100                   | 449 + 1  | 449 + 1      | 998 + 2      | 1998 + 2      |
| 100–200                | 449 + 1  | 449 + 1      | 998 + 2      | 1990 + 10     |
| 200–300                | 449 + 1  | 995 + 5      | 1495 + 5     | 1980 + 20     |
| 300–400                | 495 + 5  | 1490 + 10    | 2490 + 10    | 2450 + 50     |

\* Both intravenous infusion and local administration of meropenem were Q12h dosing.

<sup>#</sup> MIC = minimum inhibitory concentration.

As demonstrated by previous data, a 2-compartmental model best represents plasma meropenem concentration-time data in elderly patients or in adult patients with febrile neutropenia (Ohata et al., 2011; Usman et al., 2017). Initially, the CSF was considered as the peripheral compartment, but the CSF concentration-time profile could not be well captured. Because CSF was directly linked to blood circulation, CSF was considered a single compartment. A variety of conditions are commonly treated by placing an external CSF catheter to drain CSF and to reduce the intracranial pressure (Weisenberg et al., 2016). The outflow of CSF from the drain tube may be the main elimination pathway of meropenem in CSF, therefore, a new parameter  $CL_{CSF}$  was added into the structure model to describe the drug loss via the drainage tube. Based on the three-compartment model with first-order elimination (CL and  $CL_{CSF}$ ), the plasma and CSF concentrations were fit simultaneously and the predicted values supported the observations well (Fig. 2). A significant positive relationship between drainage volume and  $CL_{CSF}$  was observed in the final pharmacokinetic model, indicating the incorporation of  $CL_{CSF}$  in the model was valid.

CSF penetration ratio (drug amount penetrated into CSF divided by intravenous dose) is a useful measure to characterize based on the data from this study. However, as both intravenous and intrathecal administration were applicable in this study. Two sources might introduce meropenem into the CSF after drug administration. Intrathecal administration being a source which introduces meropenem to the CSF can actually be resolved by performing simulations in which meropenem is only administered via the intravenous route.

The normal circulation of CSF can be described as follows (Bradley et al., 2016): CSF flows from the lateral ventricle to the third ventricle through the interventricular foramen, or foramen of Monroe. The cerebral aqueduct, the aqueduct of Sylvius, connects the third and fourth ventricles. CSF flows into the subarachnoid space through the foramina of Luschka and the foramen of Magendie, and subsequently circulates through the freely communicating subarachnoid cisterns at the base of the brain. From the cisterns, a large amount of CSF is directed upward over the cerebral hemispheres with a smaller amount passing downward the spinal cord. A neurosurgical operation disrupts the normal circulation of CSF.

**Table 3**

Percent probabilities of PK/PD target attainment\* for meropenem dosing regimens by drainage volume and MIC value for postoperative neurosurgical patients with intracranial infections.

| Drainage volume (ml/d) | Percent probabilities of PK/PD target attainment for meropenem dosage regimens [IV dose (mg) + local dose (mg)] by drainage volume and MIC value shown in Table 2 |              |              |               |
|------------------------|---|--------------|--------------|---------------|
|                        | MIC = 2 mg/L  | MIC = 4 mg/L | MIC = 8 mg/L | MIC = 16 mg/L |
| <100                   | 86.9%   | 86.5%        | 85.6%        | 83.6%         |
| 100–200                | 87.5%   | 87.4%        | 86.4%        | 84.5%         |
| 200–300                | 90.9%   | 89.8%        | 87.6%        | 85.5%         |
| 300–400                | 91.6%   | 90.1%        | 88.1%        | 85.6%         |

\* Based on achieving 100% T > MIC in CSF.

The CSF circulation process and the location of the drainage tube placement are key factors influencing the drug distribution in CSF. In this study, local intrathecal administration may not spread to infection sites due to the CSF circulation obstruction. Therefore, the simultaneous intravenous and local administrations were considered to be optimal treatment. Initially, we speculated that the drainage position (ventricles, subdural and operational cavity drainage) may be one of the significant covariates, however, no impact was observed after model development. This result may be due to most of the patients in the limited cohort having a drainage position in the operational cavity (~67%).

Meropenem 10 mg was given via the drainage tube, and the tube was clamped off for 15 minutes. After the clamp re-opening, we observed that the retained CSF outflowed instantaneously. We speculated that this coupled with the poor CSF backflow to the brain area caused a high drug concentration in the CSF outflow, resulting in a certain amount of drug loss. The actual dose of meropenem that went into the CSF may be less than the theoretical dose. Because the amount of instantaneous CSF outflow was not accurately recorded, we could not obtain an accurate measure for the amount of drug loss. Drug loss may lead to a deviation from the calculated model parameters (the estimated  $CL_{CSF}$  was greater than the actual drainage volume, and the calculated  $V_{CSF}$  was greater than the true volume of CSF).

Due to postoperative patients' frail physical conditions at the time of the blood and CSF draw, certain specimens were not able to be collected. For sparse data, conventional pharmacokinetic studies are difficult as adequate blood sampling is not possible. The nonlinear mixed effects modeling approach is appropriate in this group of patients.

Several limitations of this study should be considered: 1) the sample size was relatively small and a larger study is needed to confirm the study conclusions; 2) meropenem loss after the clamp re-opening provided important information for parameter estimation, and this problem should be addressed in a follow-up study; and 3) well-known covariates, such as creatinine clearance, body weight, were not added in the final model due to a homogeneous and small cohort.

In summary, we developed the meropenem plasma and CSF population pharmacokinetic model in postoperative neurosurgical patients treated with both intravenous and intrathecal administration. Drainage volume (mL/d) was identified as a significant covariate influencing the CSF concentration. Simulation was performed based on the final pharmacokinetic model. Findings based on these simulated data suggest that and intravenous and local meropenem doses should increase as MIC and daily CSF drainage volume increase. These study results may be useful for clinicians to select an optimal meropenem dosing regimen for the treatment of patients with intracranial infections.

Supplementary data to this article can be found online at <https://doi.org/10.1016/j.diagmicrobio.2018.08.003>.

## Conflict of Interest

None declared.

## Funding

This work was supported by grants from National Natural Science Foundation of China (81503157), Beijing Municipal Administration of Hospitals' Youth Programme (QML20170506), National Key Research and Development Project (2017YFC1310900), and Beijing Municipal Administration of Hospitals (ZYLX201808).

## Acknowledgements

We would like to thank the Intensive Care Unit nurses, for their help for collecting the samples.

## References

- Beer R, Lackner P, Pfausler B, Schmutzhard E. Nosocomial ventriculitis and meningitis in neurocritical care patients. *J Neurol* 2008;255(11):1617–24.
- Blassmann U, Roehr AC, Frey OR, Vetter-Kerkhoff C, Thon N, Hope W, et al. Cerebrospinal fluid penetration of meropenem in neurocritical care patients with proven or suspected ventriculitis: a prospective observational study. *Crit Care* 2016;20(1):343.
- Bradley WG, Haughton V, Mardal KA. Cerebrospinal fluid flow in adults. *Handb Clin Neurol* 2016;135:591–601.
- Chung EK, Cheatham SC, Fleming MR, Healy DP, Kays MB. Population pharmacokinetics and pharmacodynamics of Meropenem in nonobese, obese, and morbidly obese patients. *J Clin Pharmacol* 2017a;57(3):356–68.
- Chung DY, Leslie-Mazwi TM, Patel AB, Rordorf GA. Management of external ventricular drains after subarachnoid hemorrhage: a multi-institutional survey. *Neurocrit Care* 2017b;26(3):356–61.
- Li C, Du X, Kuti JL, Nicolau DP. Clinical pharmacodynamics of meropenem in patients with lower respiratory tract infections. *Antimicrob Agents Chemother* 2007;51(5):1725–30.
- Li X, Wu Y, Sun S, Mei S, Wang J, Wang Q, et al. Population pharmacokinetics of vancomycin in postoperative neurosurgical patients. *J Pharm Sci* 2015;104(11):3960–7.
- Li X, Wu Y, Sun S, Zhao Z, Wang Q. Population pharmacokinetics of vancomycin in postoperative neurosurgical patients and the application in dosing recommendation. *J Pharm Sci* 2016;105(11):3425–31.
- Li X, Sun S, Ling X, Chen K, Wang Q, Zhao Z. Plasma and cerebrospinal fluid population pharmacokinetics of vancomycin in postoperative neurosurgical patients after combined intravenous and intraventricular administration. *Eur J Clin Pharmacol* 2017;73(12):1599–607.
- Li X, Sun S, Wang Q, Zhao Z. Population pharmacokinetics of combined intravenous and local intrathecal administration of meropenem in aneurysm patients with suspected intracranial infections after craniotomy. *Eur J Drug Metab Pharmacokinet* 2018;43(1):45–53.
- Lu C, Zhang Y, Chen M, Zhong P, Chen Y, Yu J, et al. Population pharmacokinetics and dosing regimen optimization of Meropenem in cerebrospinal fluid and plasma in patients with meningitis after neurosurgery. *Antimicrob Agents Chemother* 2016;60(11):6619–25.
- National Nosocomial Infections Surveillance S. National Nosocomial Infections Surveillance (NNIS) system report, data summary from January 1992 through June 2004, issued October 2004. *Am J Infect Control* 2004;32(8):470–85.
- Ohata Y, Tomita Y, Nakayama M, Tamura K, Tanigawara Y. Optimal treatment schedule of meropenem for adult patients with febrile neutropenia based on pharmacokinetic-pharmacodynamic analysis. *J Infect Chemother* 2011;17(6):831–41.
- Remes F, Tomas R, Jindrak V, Vanis V, Setlik M. Intraventricular and lumbar intrathecal administration of antibiotics in postneurosurgical patients with meningitis and/or ventriculitis in a serious clinical state. *J Neurosurg* 2013;119(6):1596–602.
- Segal-Maurer S, Mariano N, Qavi A, Urban C, Rahal Jr JJ. Successful treatment of ceftazidime-resistant *Klebsiella pneumoniae* ventriculitis with intravenous meropenem and intraventricular polymyxin B: case report and review. *Clin Infect Dis* 1999;28(5):1134–8.
- Shi ZH, Xu M, Wang YZ, Luo XY, Chen GQ, Wang X, et al. Post-craniotomy intracranial infection in patients with brain tumors: a retrospective analysis of 5723 consecutive patients. *Br J Neurosurg* 2017;31(1):5–9.
- Shofty B, Neuberger A, Naffaa ME, Binawi T, Babitch T, Rappaport ZH, et al. Intrathecal or intraventricular therapy for post-neurosurgical gram-negative meningitis: matched cohort study. *Clin Microbiol Infect* 2016;22(1):66–70.
- Tsai D, Stewart P, Goud R, Gourley S, Hewagama S, Krishnaswamy S, et al. Optimising meropenem dosing in critically ill Australian indigenous patients with severe sepsis. *Int J Antimicrob Agents* 2016;48(5):542–6.
- Tsimogianni A, Alexandropoulos P, Chantziara V, Vassi A, Micha G, Lagiou F, et al. Intrathecal or intraventricular administration of colistin, vancomycin and amikacin for central nervous system infections in neurosurgical patients in an intensive care unit. *Int J Antimicrob Agents* 2017;49(3):389–90.
- Tunkel AR, Hartman BJ, Kaplan SL, Kaufman BA, Roos KL, Scheld WM, et al. Practice guidelines for the management of bacterial meningitis. *Clin Infect Dis* 2004;39(9):1267–84.
- Usman M, Frey OR, Hempel G. Population pharmacokinetics of meropenem in elderly patients: dosing simulations based on renal function. *Eur J Clin Pharmacol* 2017;73(3):333–42.
- Weisenberg SH, TerMaath SC, Seaver CE, Killeffer JA. Ventricular catheter development: past, present, and future. *J Neurosurg* 2016;125(6):1504–12.
- Wu Y, Kang J, Wang Q. Drug concentrations in the serum and cerebrospinal fluid of patients treated with norvancomycin after craniotomy. *Eur J Clin Microbiol Infect Dis* 2017;36(2):305–11.
- Zhang Y, Zhang J, Chen Y, Yu J, Cao G, Wu X, et al. Evaluation of Meropenem penetration into cerebrospinal fluid in patients with meningitis after neurosurgery. *World Neurosurg* 2017;98:525–31.